

subcellular distributions, with high selectivity for synaptic vesicles²² or the relevant functional pools of synaptic vesicles, would help to further reduce background fluorescence due to nonsynaptic organelles or nonfunctional vesicle pools.

[39] Studying Organelle Physiology with Fusion Protein-Targeted Avidin and Fluorescent Biotin Conjugates

By MINNIE M. WU, JUAN LLOPIS, STEPHEN R. ADAMS,
J. MICHAEL MCCAFFERY, KEN TETER, MARKKU S. KULOMAA,
TERRY E. MACHEN, HSIAO-PING H. MOORE, and ROGER Y. TSIEH

Introduction

We have developed and used a novel method for studying the luminal pH of specific cellular organelles: a membrane-permeable, pH-sensitive fluorescein-biotin derivative is targeted to specific organelles expressing avidin chimera proteins. Until recently, the major hurdle to studying organelle pH in live cells had been the lack of appropriate methods for targeting pH probes to specific organelles. Several groups have now targeted pH dyes specifically to the Golgi, *trans*-Golgi network (TGN), and endoplasmic reticulum (ER) of live, intact cells by using the following methods: microinjection of cells with pH dye-filled liposomes, which appeared to fuse preferentially with the Golgi,¹ targeting a fluorescently labeled bacterial toxin to the Golgi or ER via retrograde transport,²⁻⁴ and expressing pH-sensitive green fluorescent protein (GFP) mutants in specific organelles.⁵⁻⁷ All these methods have provided important contributions to the understanding of the regulation of organelle pH; however, each approach has certain drawbacks. Microinjection of dye-containing liposomes is technically difficult, and fusion of the liposomes to Golgi membranes may result in perturbation of

¹ O. Seksek, J. Biwersi, and A. S. Verkman, *J. Biol. Chem.* **270**, 4967 (1995).

² J. H. Kim, C. A. Lingwood, D. B. Williams, W. Furuya, M. F. Manolson, and S. Grinstein, *J. Cell Biol.* **134**, 1387 (1996).

³ N. Demaurex, W. Furuya, S. D'Souza, J. S. Bonifacino, and S. Grinstein, *J. Biol. Chem.* **273**, 2044 (1998).

⁴ J. H. Kim, L. Johannes, B. Goud, C. Antony, C. A. Lingwood, R. Daneman, and S. Grinstein, *Proc. Natl. Acad. Sci. U.S.A.* **95**, 2997 (1998).

⁵ M. Kneen, J. Farinas, Y. Li, and A. S. Verkman, *Biophys. J.* **74**, 1591 (1998).

⁶ J. Llopis, J. M. McCaffery, A. Miyawaki, M. G. Farquhar, and R. Y. Tsien, *Proc. Natl. Acad. Sci. U.S.A.* **95**, 6803 (1998).

⁷ G. Miesenböck, D. A. De Angelis, and J. E. Rothman, *Nature (London)* **394**, 192 (1998).

the ionic composition and function of the Golgi. Using fluorescently labeled bacterial toxins to measure pH is more advantageous, but globotriaosyl ceramide, the cell surface glycolipid necessary for toxin internalization, is not expressed on all cell types. Also, the Golgi localization of the pH probe relies on the kinetics of retrograde transport of the toxin, and signal from other, adjacent organelles in the secretory pathway cannot be eliminated. Furthermore, the toxin-derived pH probe labels only compartments that can be reached by retrograde transport (e.g., endosomes, Golgi, and ER). Organelles such as secretory granules and mitochondria remain inaccessible. Targeting pH-sensitive GFP mutants to cellular compartments is the least invasive and most specific method for studying organelle pH, but most GFPs are nonratiometric, and thus prone to artifacts due to changes in focus or dye concentration, and they do not exhibit optimal pK_a values for all organelle environments.

We developed a new method for measuring organelle pH because we wished to use ratiometric dyes with pK_a values close to the pH found in the Golgi and ER (and other organelles). A fluorescein-biotin-based ratiometric pH dye (Flubi-2) with pK_a 6.7 was targeted as a nonfluorescent membrane-permeable form (Flubida-2) to the ER and Golgi, using avidin chimera proteins. This chapter describes how the avidin chimera proteins were expressed in specific organelles of mammalian cells, the synthesis and characteristics of the Flubida dyes, and the methods used for labeling avidin-containing compartments with Flubi dyes and then studying pH regulation in mammalian organelles.

Experimental Strategy and Construction of Avidin-KDEL and Sialyltransferase-Avidin Plasmids

The strategy for targeting Flubi-2 to organelles is shown in Fig. 1A and C. We constructed avidin chimera plasmids that would express avidin chimera proteins localized to specific intracellular compartments on the basis of their targeting sequences. Cells expressing these avidin chimera proteins were loaded with Flubida-2 (Fluorescein biotin diacetate-2, the membrane-permeable, nonfluorescent ester form of Flubi-2), which accumulates in the cell after esterase hydrolysis of the charge-masking acetate esters. The high affinity of biotin for avidin retains the dye in the cellular compartment expressing the chimera while unbound dye leaks out of other cellular compartments during a subsequent washing step. All the chimera proteins were constructed so that the avidin portion would be in the organelle lumen. The targeting sequence for sialyltransferase (ST), a *trans*-Golgi resident enzyme, was fused to avidin (AV) to make the single-pass transmembrane ST-avidin fusion protein (ST-AV), which was used to target

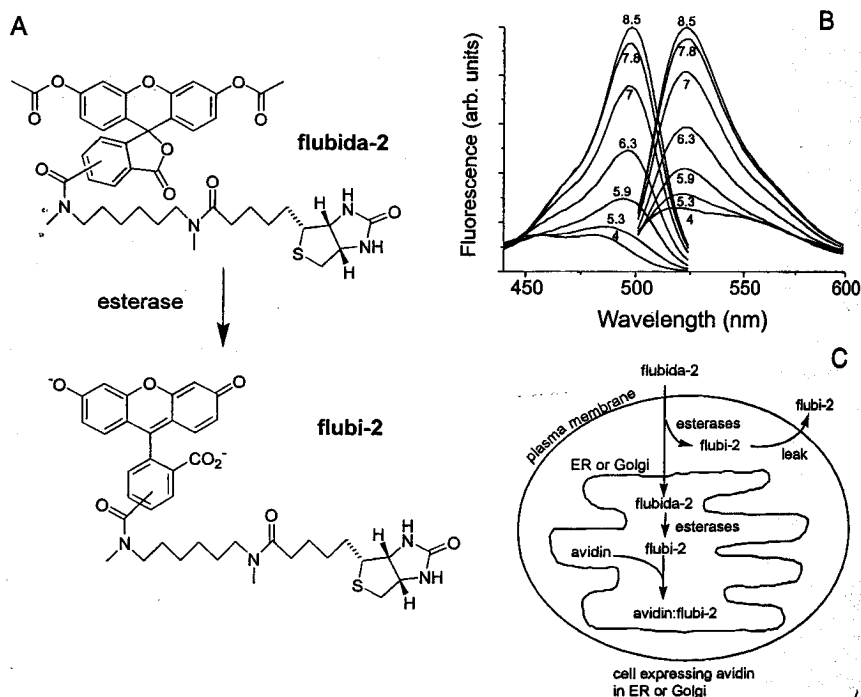


FIG. 1. A strategy for targeting pH-sensitive dyes to organelles. (A) Chemical structures of Flubi-2 and its membrane-permeable, nonfluorescent ester form, Flubida-2. (B) *In vitro* pH dependence of the excitation spectrum (emission, 530 nm) and emission spectrum (excitation, 480 nm) of Flubi-2. (C) Organelle-specific avidin chimera proteins were transiently expressed in HeLa cells. Transfected cells were loaded with 2–4 μ M Flubi-2 overnight (at least 10 hr), before chasing with normal growth medium (at least 2 hr) to minimize background fluorescence. Labeled cells are then ready for ratio imaging experiments.

Flubi dyes to the Golgi lumen. Soluble avidin (AV) was appended with the C-terminal tetrapeptide KDEL, an ER retrieval motif, to give soluble AV-KDEL, which was used to target Flubi dyes to the ER lumen.

Sialyltransferase was polymerase chain reaction (PCR) amplified from human α -2,6-sialyltransferase-avidin (B. Seed, Massachusetts General Hospital, Boston, MA), using primers (5'-cgcggaagcttgccaccatgattcacacacactg-3' and 5'-cgcgggcgatcctgggtgctgcttgagga-3') that introduced 5' *Hind*III and 3' *Bam*HI restriction sites, allowing isolation of a fragment containing the cytosolic, transmembrane, and truncated luminal domains of ST. This truncated ST contains the 17-amino acid sequence suf-

ficient for Golgi retention.⁸ Avidin was PCR amplified from chicken avidin (courtesy of M. Kulomaa, University of Tampere, Finland), using primers (5'-cgcggggatcccgccagaaagtgtctgtg-3' and 5'-cgcgggggcgccgct cactctctgtgtgtgc-3') that allowed isolation of full-length avidin with 5' *Bam*HI and 3' *Not*I restriction sites. ST and AV were triple-ligated into pCDM8 plasmid (courtesy of B. Seed), using *Hind*III, *Bam*HI, and *Not*I restriction sites. Avidin-KDEL (AV-KDEL) was PCR amplified from chicken avidin with primers (5'-atccaagctgtgtcagagatggtgc-3' and 5'-taatg-gatcctcacagctgtctttctcttctgtgtgcgagcg-3') that appended the KDEL tetrapeptide sequence to the C terminus of avidin and allowed cloning of AV-KDEL by 5' *Hind*III and 3' *Bam*HI restriction sites into the pCDNA3 vector (InVitrogen, San Diego, CA).

Expression of Avidin-KDEL and Sialyltransferase-Avidin in Mammalian Cells

AV-KDEL and ST-AV were expressed in HeLa cells, which were cultured at 37° in Dulbecco's modified Eagle's medium (DMEM; Biowhitaker, Walkersville, MD) supplemented with 10% (v/v) fetal calf serum (Sigma, St. Louis, MO), penicillin (20 U/ml), and streptomycin (20 mg/ml) (Biowhitaker) and grown in the presence of air-6% CO₂. HeLa cells were transiently transfected with either AV-KDEL or ST-AV DNA by electroporation. Cells from a 50–75% confluent 10-cm dish were trypsinized, washed twice, and resuspended in 0.8 ml of ice-cold sucrose buffer [270 mM sucrose, 7 mM sodium phosphate buffer (pH 7.4), 1 mM MgCl₂]. Ten micrograms of DNA (AV-KDEL or ST-AV) was added to the cell suspension just prior to electroporation (GenePulser; Bio-Rad, Hercules, CA) in ice-cold 0.4-mm gap cuvettes (Bio-Rad) at 500 V, 200 Ω, 25 μF. After electroporation, cells recovered on ice for 10 min before being replated in normal growth medium. Peak expression of AV-KDEL and ST-AV for transiently transfected HeLa cells was 48 to 72 hr posttransfection. We also generated a cell line stably expressing AV-KDEL by selection with G418. Neither transient nor stable expression of avidin chimera proteins appeared to affect cell health or viability, because transfected cells were similar in morphology and growth rate to untransfected cells. In addition to the AV-KDEL and ST-AV chimera proteins, we also constructed avidin chimera proteins that localize to the ER-Golgi intermediate compartment (ERGIC-avidin), medial-Golgi (MG160-avidin), and secretory granules (proopiomelanocortin-avidin).

The intracellular localization of the ER- and Golgi-localized avidin

⁸ S. H. Wong, S. H. Low, and W. Hong, *J. Cell Biol.* **117**, 245 (1992).

chimera proteins was confirmed by fluorescence staining [with fluorescein isothiocyanate (FITC)-biotin or fluorescent antibodies] and by electron microscopy. For fluorescence staining, 48 to 60 hr posttransfection, cells plated on 22-mm coverslips were washed twice with phosphate-buffered saline (PBS), fixed in 4% (w/v) paraformaldehyde for 20 min at room temperature, and permeabilized in ice-cold 100% methanol for 15 sec. Cells were incubated for 30 min in 1% (w/v) bovine serum albumin (BSA)-PBS before incubation in either FITC-biotin (Molecular Probes, Eugene, OR) or in goat anti-avidin D antibody (Vector Laboratories, Burlingame, CA) for 1 hr at room temperature. Cells stained with FITC-biotin were then rinsed once with PBS and mounted on slides with a nonbleach reagent (KPL mounting medium; Kirkegaard & Perry, Gaithersburg, MD) and viewed with a Zeiss (Oberkochen, Germany) Axiophot fluorescence microscope with $\times 63$ oil objective. For electron microscopy, 48 to 60 hr posttransfection, cells were washed with PBS, fixed in 4% (w/v) paraformaldehyde-0.05% (v/v) glutaraldehyde for 1 hr at room temperature, permeabilized with 0.1% (w/v) saponin in 1% (w/v) BSA-PBS, and sequentially incubated in primary goat anti-avidin antibody followed by horseradish peroxidase-conjugated secondary antibody diluted in 1% (w/v) BSA-PBS containing 0.1% (w/v) saponin for 1 hr each. The cells were washed in 0.1 M cacodylate-HCl, pH 7.4, followed by fixation in 2% (v/v) glutaraldehyde contained in 0.1 M cacodylate-HCl, pH 7.4, for 1 hr, incubation in diaminobenzidine, postfixation in 0.1 M cacodylate containing 1% (w/v) OsO_4 and 1% (w/v) KFeCN , and then processing as previously described.⁹ Figure 2 shows the intracellular localization of AV-KDEL by immunoperoxidase staining, visualized by electron microscopy.

Rescue of Mislocalized Avidin Chimera Proteins

Oligomerization of avidin due to the well-known homotetrameric interactions appeared not to affect targeting of AV-KDEL or ST-AV.¹⁰ However, avidin oligomerization may become problematic with some constructs. For example, we have found that avidin-furin and avidin-P-selectin were not targeted, as expected, to the TGN and secretory granules, respectively, in neuroendocrine (AtT-20) cells, but to the nuclear envelope and large, membrane-bound vesicles, which may have been ER derived. One possibility is that the mistargeting was due to aggregate formation when an oligomeric targeting signal (P-selectin can form hexamers, and furin forms dimers) was combined with tetrameric avidin. If so, overexpression of native

⁹ J. M. McCaffery and M. G. Farquhar, *Methods Enzymol.* **257**, 259 (1995).

¹⁰ N. M. Green, *Adv. Protein Chem.* **29**, 85 (1975).

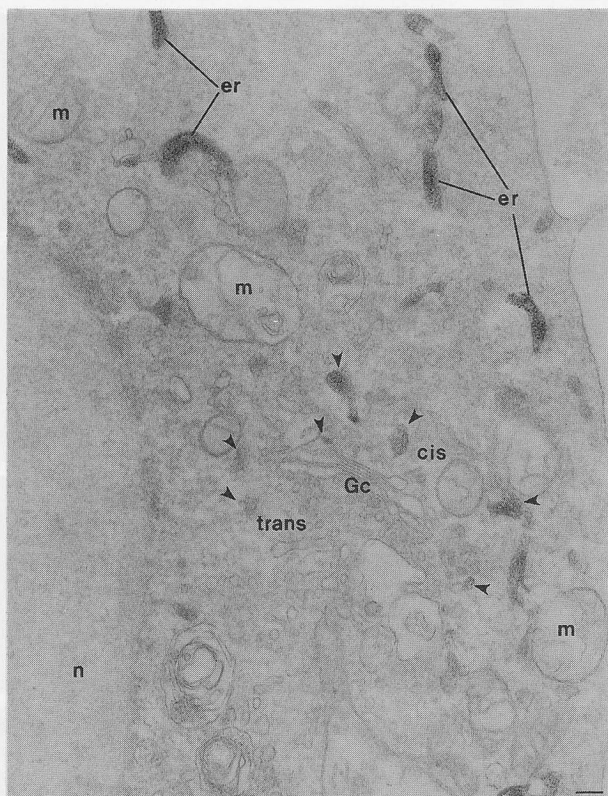


FIG. 2. Immunoperoxidase staining of AV-KDEL. NRK cells expressing AV-KDEL were immunoperoxidase labeled with a polyclonal antibody against avidin and then visualized by electron microscopy. Extensive labeling is seen confined to the ER (solid lines) and dilated rims of the *cis*-Golgi network (arrowheads) but is not detected on the *trans*-most Golgi cisternae, consistent with previously reported KDEL localizations. Bar: 0.2 μm .

soluble avidin (not fused to any membrane-bound targeting sequence) should compete with the avidin chimera proteins for tetramerization and prevent the formation of mistargeted aggregates. To test this, we made a recombinant adenovirus carrying a tetracycline-repressible soluble avidin construct. Expression of this virus in AtT-20 cells rescued the mislocalization of avidin-furin (and avidin-P-selectin, not shown). Cells expressing avidin-furin alone showed aberrant localization of FITC-biotin staining to the nuclear envelope, ER, and vesicular structures (Fig. 3B), which differed from the TGN localization of native furin (Fig. 3A). Coexpression of avidin-furin with soluble avidin resulted in correct localization to the TGN (Fig. 3C); the observed FITC-biotin staining was due to membrane-

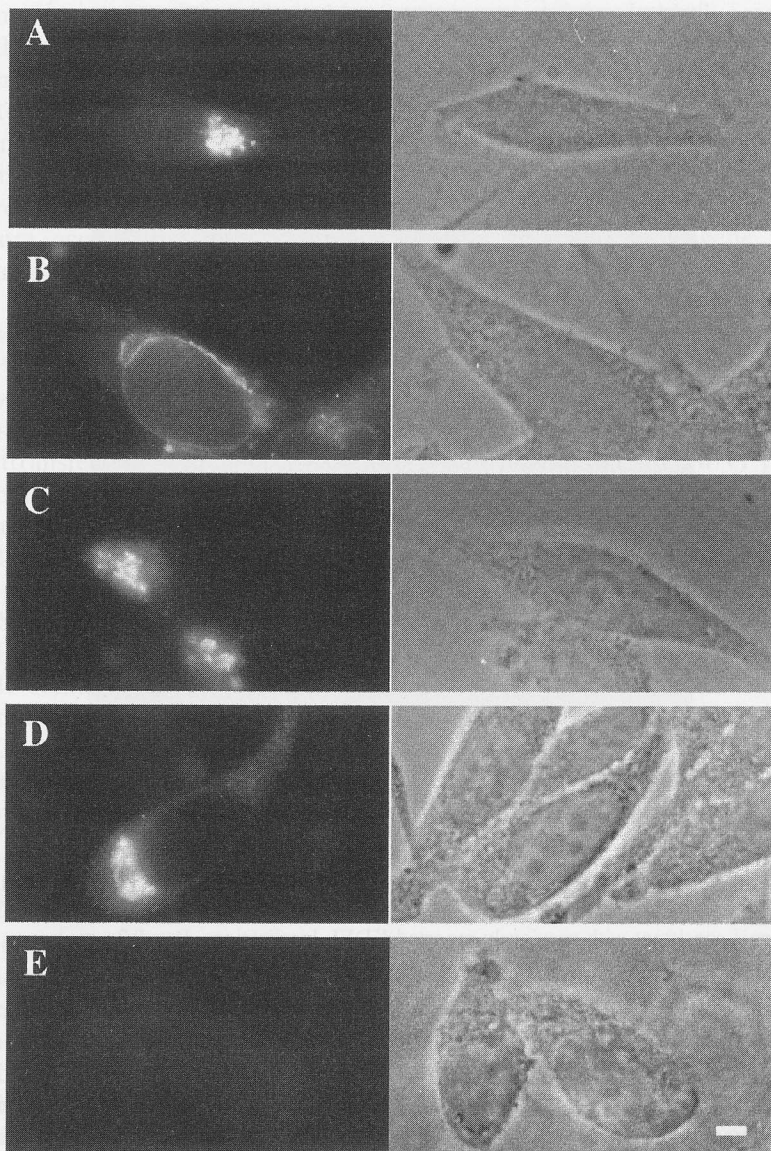


FIG. 3. Rescue of mislocalized avidin-furin. (A) The normal TGN localization of furin is shown in fixed, permeabilized, and stained (with anti-FLAG antibody) AtT-20 cells expressing an FLAG-tagged, full-length Furin protein. (B) Avidin-furin in AtT-20 cells is mislocalized to the nuclear envelope, ER, and vesicular structures. Cells were fixed, permeabilized, and stained with FITC-biotin. (C) When avidin-furin was coexpressed with soluble avidin, using a recombinant adenovirus, and treated with cycloheximide (100 $\mu\text{g}/\text{ml}$) for 3 hr, avidin-furin

bound avidin–furin and not soluble avidin, because in this experiment the cells were pretreated with cycloheximide (100 $\mu\text{g/ml}$) for 3 hr to clear soluble avidin from the secretory pathway (see below).

We performed control experiments (Fig. 3D and E) to ensure that the staining in the rescued AtT-20 cells was not due to soluble avidin alone. Untransfected cells were infected with avidin–adenovirus and then fixed, permeabilized, and stained or, alternatively, treated with cycloheximide (100 $\mu\text{g/ml}$) to inhibit new protein synthesis before being fixed, permeabilized, and stained. Control cells that had been infected with avidin–adenovirus showed FITC–biotin staining in a perinuclear structure, probably the Golgi, on its way to being secreted (Fig. 3D). After a 3-hr cycloheximide treatment, all the soluble avidin was chased out of the cells (Fig. 3E).

Thus, as is the case with all chimera proteins, careful controls should be performed to assure proper organelle localization of the avidin chimera proteins. In some cases in which avidin chimera proteins become mistargeted due to oligomerization, correct targeting can be achieved by the rescue strategy described here or by constructing avidin chimera proteins with a mutant, monomeric avidin (M. Kulomaa, unpublished results, 1999).

Synthesis and *in Vitro* Characterization of Flubi Dyes

The chemical structures of the Flubi dyes are shown in Fig. 4. All the dyes are membrane permeable and can be used in the ratiometric mode. Four Flubi dyes, each with a different pK_a , allow measurements of pH in organelles with different pH values by matching the pK_a of the indicator dye with the pH environment of the organelle lumen. The range of pK_a values of the Flubi dyes allow measurements in organelles that range in luminal pH from 7.2 (ER) to 4.5 (lysosomes). The Flubi-2 dye was advantageous for studies of pH regulation in the ER ($\sim\text{pH}$ 7.2) and Golgi ($\sim\text{pH}$ 6.4), because it had a pK_a of about 6.5 (see below, pK_a 6.8 for ER *in situ*, pK_a 6.6 for Golgi *in situ*). Another advantage of using the ratiometric Flubi dyes compared with nonratiometric pH indicators such as most pH-sensitive GFP mutants is that changes in fluorescence intensity due to variation in

was correctly localized to the TGN, as detected by FITC–biotin staining. (D) Control cells that had been infected with the avidin adenovirus alone showed FITC–biotin staining in a perinuclear structure, probably the Golgi, on its way to being secreted. (E) After avidin-infected control cells [e.g., cells in (D)] were treated with cycloheximide (100 $\mu\text{g/ml}$) for 3 hr, all the soluble avidin was chased out of the cells, resulting in no specific FITC–biotin staining. Bar: 5 μm .

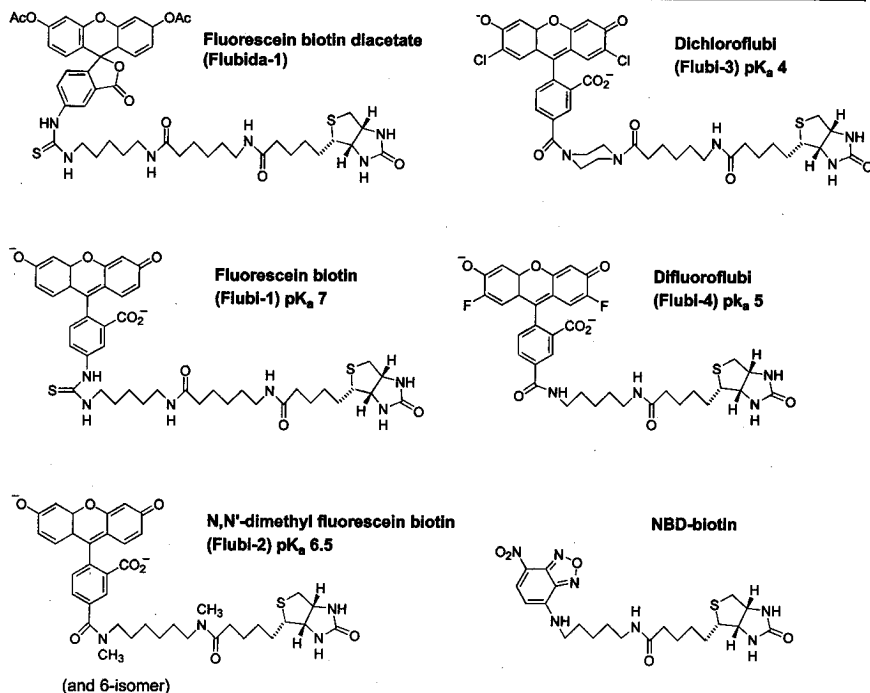


FIG. 4. Chemical structures of the Flubi dyes. Flubida-1 is the nonfluorescent and membrane-permeable form of Flubi-1. Corresponding structures for Flubida-2, -3, and -4 are not illustrated but contain the fluorescein moiety in the same acetylated and lactonized form. The pK_a values refer to the apparent H^+ dissociation constants for the avidin-bound dyes measured *in vitro*.

path length or dye concentration are eliminated, because these factors affect both the pH-sensitive and pH-insensitive wavelengths equally. The Flubi dyes have an excitation spectrum with a pH-sensitive wavelength at 490 nm and pH-insensitive wavelength at 440 nm (see Fig. 1B for the pH dependencies of the excitation and emission spectra of Flubi-2 *in vitro*). Hydrolysis of Flubida-2 to Flubi-2 inside the cell occurs in the cytosol and organelles, as demonstrated by the appearance of the fluorescent species (Flubi-2) on cleavage of the acetate groups.

Synthesis of Flubida-1

Fluorescein biotin (1.8 mg, 2.2 μ mol) was suspended in acetic anhydride (2 ml), refluxed until a colorless solution was formed (about 2 hr), and evaporated. Thin-layer chromatography (TLC) [SiO₂-10% (v/v) methanol-

CHCl_3] revealed two major products that turned fluorescent on heating the plate. Only the least polar product was positive when sprayed with a biotin-specific stain.¹¹ Reactions with model compounds indicated that these reaction conditions resulted in partial acylation of the biotin ureido group, giving a product that did not test positive for biotin and did not bind avidin. The mixture was used without further purification.

Synthesis of Flubida-2

N,N'-Dimethyl-(6-aminohexyl)biotinamide. *N,N'*-Dimethylhexane-2,6-diamine (65 μl , 0.37 mmol; Aldrich, Milwaukee, WI) was added with rapid stirring to a solution of succinimidyl D-biotin (25 mg, 0.073 μmol) in dry dimethyl fluoride (DMF, 0.5 ml) under argon. After 2 hr at room temperature, the white solid was removed by centrifugation, the supernatant was evaporated to dryness and redissolved in absolute ethanol, and the product was separated by preparative layer chromatography [Analtech (Newark, DE) SiO_2 G plate eluted with butanol-hydroxyacetate- H_2O (12:3:5, by volume)] and visualized at one edge with biotin spray¹¹ (R_f 0.4). The product was extracted twice with hot ethanol and evaporated to dryness. Silica was removed by centrifugation through a 0.2- μm pore size filter after dissolution in a few milliliters of 20% (v/v) methanol- CHCl_3 . Evaporation of the filtrate gave an off-white solid. Yield, 20 mg (74%). $^1\text{H-NMR}$ (200 MHz, δ ppm, CDCl_3 - CD_3OD) 1.0–1.6 (m's, 14H, $-\text{CH}_2-$), 2.16 (t, 2H, $-\text{CH}_2-\text{CO}$), 2.47 (s, 3H, $\text{MeHN}-$), 2.55 (d, 2H, biotin S- CH_2), 2.71 (s, MeN-CO), 2.75 (s, mm, CH_2NH , biotin S- CH_2), 2.97 (m, 1H, biotin S- $\text{CH}-$), 3.13 (t, partially obscured by CD_3OD peaks, $\text{CH}_2\text{-N-CO}$), 4.1–4.4 (multiplets partially obscured by water peak, biotin N- CH). Electrospray mass spectrum: 371.3 ($\text{M}+1$); calc. 371.5.

Flubida-2. *N,N'*-Dimethyl-(6-aminohexyl) biotinamide (7.5 mg, 20 μmol) was dissolved in 20% (v/v) methanol- CHCl_3 (1 ml) and 5 (and 6)-carboxyfluorescein; succinimidyl ester (15 mg, 33 μmol) dissolved in dry DMF (1 ml) was added, followed by *N,N* Diisopropyl-ethylamine (DIEA) (100 μl). The red solution was stirred overnight, evaporated, and resuspended in acetic anhydride (2 ml) and pyridine (5 μl) and heated at 60° with stirring for 20 min. The colorless reaction mixture was evaporated and the product separated by SiO_2 chromatography [5–10% (v/v) methanol- CHCl_3] as a gummy white solid. Yield, 4 mg (25%). $^1\text{H-NMR}$ (200 MHz, δ ppm, CDCl_3 - CD_3OD) was complex, containing peaks characteristic for a 5 (and 6)-substituted fluorescein diacetate, a *N,N'*-dimethylhexanediamide, and biotin. Electrospray mass spectrum: 813.3 ($\text{M} + 1$); calc. 813.9.

¹¹ D. B. McCormick and J. A. Roth, *Methods Enzymol.* **18A**, 383 (1970).

Flubi-2. Flubida-2 [10 μ l of 3.5 mM solution in dimethyl sulfoxide (DMSO)] was diluted in methanol (50 μ l), and aqueous 1 M KOH (10 μ l) was added at room temperature. After 30 min, the brightly fluorescent solution was neutralized with 1 M HEPES (20 μ l), evaporated, and redissolved in H₂O (35 μ l).

Synthesis of Flubida-3

t-Butyl *O,O*-Diacyetyl 2',7'-dichlorofluorescein-(5,6)-carboxamidopiperazine-4-carboxylate. 5-Carboxy-2',7'-dichlorofluorescein diacetate (132 mg, 0.25 mmol) was suspended in dry CH₂Cl₂ (0.5 ml) under argon. After adding 4-methyl morpholine (33 μ l, 0.3 mmol), the resulting solution was cooled to 0° and isobutyl chloroformate (36 μ l, 0.28 mmol) was added with stirring. After 15 min, *t*-butyl 1-piperazinecarboxylate (51 mg, 0.28 mmol) was added, and the reaction mixture was slowly allowed to warm up to room temperature (over 2 hr) and then evaporated. The crude product was dissolved in ethylacetate (25 ml), washed with 1 M HCl (20 ml) and brine (20 ml), dried, and evaporated to a yellow oil. After triturating with ethanol, 45 mg of starting material was recovered by filtration as a white solid. The evaporated filtrate was separated by SiO₂ chromatography by elution with ethyl acetate-hexane (30-66%, v/v) to yield the product as a white solid. Yield, 43.7 mg (25%).

Flubi 3. *t*-Butyl *O,O*-diacyetyl 2',7'-dichlorofluorescein-(5,6)-carboxamidopiperazine-4-carboxylate (10 mg, 14 μ mol) was dissolved in dry CH₂Cl₂ (1 ml) under argon and treated with trifluoroacetic acid (100 μ l) at room temperature for 2 hr. After evaporation and redissolution in methanol (1 ml) and H₂O (1 ml), the acetyl esters were removed by the addition of sufficient 1 M KOH to maintain a pH of 10-11 for about 5 min. The dark red solution was neutralized to about pH 7.5 with 1 M HCl, evaporated, and redissolved in water to make a 10 mM solution. This solution (1.25 ml, 10 mM) was mixed with a DMF solution of biotin-succinimidyl ester (1.25 ml, 10 mM) and an aqueous solution of 4-methyl morpholine (0.5 M, 125 μ l). After 72 hr at room temperature, capillary electrophoresis (20 kV, 50 mM borate, pH 8.5) indicated reaction completion, and the reaction mixture was evaporated. The resulting crude product was redissolved in aqueous sodium bicarbonate (<1 ml), filtered (0.2- μ m pore size centrifugal filter), and reprecipitated with aqueous HCl. The resulting orange solid was collected by centrifugation, washed with cold H₂O, and desiccated *in vacuo* over phosphorus pentoxide.

Flubida-3. Crude Flubi-3 free acid (5 mg, 5.9 μ mol) was suspended in acetic anhydride (2 ml) and pyridine (5 μ l) and heated at 60° for a few minutes until colorless. After evaporation, the product was dissolved in 5%

(v/v) methanol- CHCl_3 (5 ml), washed with 1 M HCl (5 ml), dried, and evaporated. The resulting material was essentially pure by TLC [10% (v/v) methanol- CHCl_3]. ^1NMR (CDCl_3 - CD_3OD ; δ ppm) 0.9–1.5 (m's, 16H), 1.9 (m, 4H) 2.17 (s, 6H, OCOCH_3), 2.52 (d, 1H), 2.72 (dd, 1H), 2.96 (t, 2H), 3.2 (m, 1-2H), 3.4 (broad m, 8H, piperazine), 4.2 (m, 2H), 6.71 (s, 1H), 7.01 (s, 1H), 7.10 (s, 1H), 7.26 (s, 1H), 7.56 (dd, 1H), 7.97 (d, 1H).

Synthesis of Flubida-4

Biotin cadaverine (1 mg, 3 μmol) and Oregon Green 5-carboxylate, succinimidyl ester (1 mg, 1.9 μmol) were suspended in dry DMF (200 μl). After brief heating to dissolve the biotin derivative, diisopropylethylamine (10 μl) was added to give a red-orange solution that was kept at room temperature for 2 hr. The reaction mixture was evaporated, suspended in acetic anhydride (1 ml) and pyridine (5 μl), and stirred until colorless. After evaporation, the product was separated by silica gel chromatography, eluting with 10% (v/v) methanol- CHCl_3 to give a colorless gum. Electro-spray mass spectrum: 807.2, calculated for $(\text{M} + 1)^+$ 807.8.

Synthesis of NBD Biotin

Biotin cadaverine (2.5 mg, 7.6 μmol) was dissolved in DMF (0.2 ml) and H_2O (0.2 ml) with gentle heating; aqueous 1 M KPO_4 (pH 7, 10 μl) and NBD chloride (4-chloro-7-nitrobenzofurazan; 2 mg, 10 μmol ; predissolved in 10 μl of dry DMF) were then added. The solution turned yellow and after 4 hr was evaporated, dissolved in 5% (v/v) methanol- CHCl_3 (25 ml), washed with aqueous 1 M KPO_4 (pH 7, 10 ml), dried, and evaporated. The product was separated by silica gel chromatography by elution with 20% (v/v) methanol- CHCl_3 .

pH Titration of Flubi-2 in the Endoplasmic Reticulum and Golgi of Intact Cells

An *in situ* calibration was performed at the end of each experiment to generate a calibration curve of 490 nm/440 nm excitation ratio (emission, 520–560 nm) versus pH, which was used to convert ratio values to pH. At the end of every experiment, cells and organelles were clamped to different pHs by perfusing calibration solutions of at least four different pHs. The calibration solutions contained (in mM): 70 NaCl, 70 KCl, 1.5 K_2HPO_4 , 1 MgSO_4 , 10 HEPES [or morpholineethanesulfonic acid (MES)], 2 CaCl_2 , and 10 glucose, were titrated to different pH values (8.2, 7.0, 6.5, 6.0, 5.5), and supplemented with 10 μM each of nigericin (Sigma, St. Louis, MO), the

K^+/H^+ exchange ionophore, and monensin (Sigma), the Na^+/H^+ exchange ionophore. We used these calibration solutions rather than the more traditional high $[K^+]$ -nigericin method because it was possible that the organelles contained different $[Na^+]$ and $[K^+]$ than the cytosol. Thus, this calibration method made no assumptions about cytosolic or organelle $[Na^+]$ and $[K^+]$ and allowed equilibration of both Na^+ and K^+ to drive the equilibration of H^+ . The 490 nm/440 nm fluorescence ratio was plotted versus pH of the calibration solution; the data were fit to a sigmoidal curve (InPlot; Graph Pad, Irvine, CA), and the resulting fit was used to convert the ratio values to pH values using Eq. (1):

$$pH = pK + \log[(R - R_{\min})/(R_{\max} - R)] \quad (1)$$

where R is the ratio of Flubi-2 fluorescence intensity excited at 490 nm/440 nm wavelength light; R_{\min} and R_{\max} are the minimum and maximum values, respectively, determined from the curve fit, and the pK is the pK_a determined from the fit. We generated average calibration curves for Flubi-2 localized in the ER (Fig. 5A) and Golgi (Fig. 5B). Flubi-2 had a similar pH dependence whether expressed in the lumen of the ER bound to AV-KDEL (Fig. 5A; pK_a 6.8 ± 0.03 SEM, $n = 13$), in the Golgi lumen bound to ST-AV (Fig. 5B, pK_a 6.6 ± 0.04 SEM, $n = 43$), or *in vitro* (Fig. 1B, the pK_a of the complex avidin-Flubi-2 separated by gel filtration using a Sephadex G25 column was 6.53).

Labeling Endoplasmic Reticulum and Golgi of Live Cells with Flubi-2

Flubida-2 was dissolved in DMSO (approximately 2 mM), mixed 1:1 with 20% (w/v in DMSO) Pluronic F-127 (Molecular Probes), and then diluted to the desired final concentration (2–4 μM) with serum-free DMEM. Thirty to 48 hr posttransfection with either AV-KDEL or ST-AV DNA, HeLa cells were rinsed once with serum-free DMEM and loaded with 2–4 μM Flubida-2 for 3–5 hr (or overnight for 10–15 hr). Background fluorescence was minimized by chasing the labeled cells with normal growth medium for at least 2 hr, to allow excess dye-biotin to exit from the cytosol. The strong avidin-biotin interaction (K_a $10^{15} M^{-1}$) ensured stable, specific avidin-Flubi-2 binding that resisted washing. Biotin starvation of the cells was not necessary before Flubida-2 loading, as staining was bright and stable.

Studying Endoplasmic Reticulum and Golgi pH with Targeted Avidin-Flubi-2 System and Fluorescence Ratio Imaging

We measured the pH of Flubi-2-loaded ER and Golgi compartments in live, intact cells by digitally processed fluorescence ratio imaging. AV-

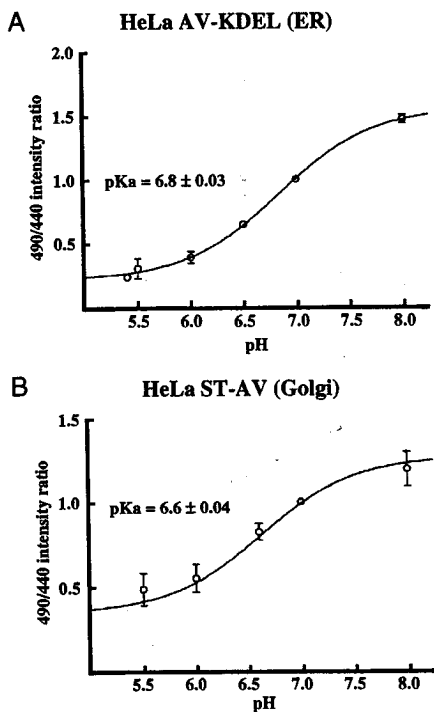


FIG. 5. *In situ* characterization of Flubi-2: 490 nm/440 nm excitation ratio (emission, 520–560 nm) versus pH_{ER} and pH_G . pH values of the ER and Golgi were monitored by the targeted avidin–Flubi method. Calibration solutions containing nigericin and monensin (10 μM each) were perfused onto cells at the end of each experiment. At least four solutions of different pH values (pH 8.2, 7.0, 6.5, 6.0, 5.5, and/or 5.0) were used. Calibration curves for both ER (A) and Golgi (B) were used to convert ratio values to pH and to determine the pK_a of the dye. The pK_a of Flubi-2 bound to AV–KDEL in the ER was 6.8 ± 0.03 SEM ($n = 13$), while Flubi-2 in the Golgi lumen bound to ST–AV had a pK_a of 6.6 ± 0.04 SEM ($n = 43$). To compare separate experiments, 490 nm/440 nm intensity ratios were normalized (pH 7 = 1.0 ratio).

KDEL- or ST–AV-expressing cells were plated on coverslips, labeled with Flubi-2, and mounted in an open perfusion chamber (at room temperature or heated to 32–37°) on an inverted IM35 Zeiss microscope with a $\times 63$ oil immersion objective. Images were transmitted to a Dage (Michigan City, IN) 68 SIT camera, which collected emission (520–560 nm; Omega Optical, Brattleboro, VT) images of the cells during alternate excitation at 490 and 440 ± 5 nm (using a Lambda-10 filter wheel; Sutter Instruments, Novato, CA). Individual images for each wavelength were averaged over eight frames by a digital image processor (Axon Imaging Workbench; Axon

Instruments, Foster City, CA) run on a 133-MHz Pentium computer (Gateway, N. Sioux City, SD). Since single experiments can require as much as 200 MB of memory, all data were written to compact disks using a CD recorder (Hi Val, Santa Ana, CA).

The avidin-Flubi method was developed with the goal of determining how pH is regulated in different compartments in the cell. We have measured the average ER pH (pH_{ER}) and Golgi pH (pH_{G}) in intact HeLa cells bathed in pH 7.4 Ringer solution (containing in mM: 141 NaCl, 2 KCl, 1.5 K_2HPO_4 , 1 MgSO_4 , 10 HEPES, 2 CaCl_2 , 10 glucose). Average pH_{ER} was 7.2 ± 0.2 SD ($n = 26$ cells), close to the average cytosolic pH (pH_{c}), measured with the widely used cytosolic pH dye BCECF-AM (7.4 ± 0.2 SD, $n = 119$); steady state pH_{G} averaged 6.4 ± 0.3 SD ($n = 46$).

Measuring Buffer Capacity and Rates of H^+ Transport across Organelle Membranes

In this section, we discuss experimental and methodological approaches required to make quantitative comparisons of rates of H^+ flux across organelle membranes. During investigations of the mechanisms that give rise to the different pH values in the ER and Golgi,¹² it became clear that the different pH values were generated in large part by having different rates of pumps and leaks for H^+ . Specifically, the ER has the same pH as the cytosol because it expresses no active H^+ -pumping ability, and there is a large leak for H^+ . The Golgi is more acidic than the ER because the Golgi has an active H^+ v-ATPase that is able to acidify the Golgi lumen despite the presence of a H^+ leak that is only three times smaller than that of the ER.

Determining H^+ leak rates from measurements of pH requires knowledge of the buffering capacity, β , as shown by Eq. (2):

$$J^{\text{H}} (\text{mmol H}^+/\text{liter}/\text{min}) = \beta (\text{mmol H}^+/\text{liter}/\text{pH}) \times \Delta\text{pH}/\text{min} \quad (2)$$

where J^{H} is the H^+ flux and ΔpH is the change in pH. We determined β for the cytosol, ER, and Golgi by measuring magnitudes of rapid increases in pH of these compartments in response to application of known concentrations (30 or 40 mM) of NH_4Cl Ringer (same as Ringer solution except 30 or 40 mM NaCl is replaced with 30 or 40 mM NH_4Cl). Because buffer capacities may be pH dependent,¹³ it is important to determine β of the Golgi and ER with bafilomycin-pretreated cells (500 nM, 2 hr) so that the baseline pH values, prior to NH_4Cl treatment, were the same for both

¹² M. M. Wu, J. Llopis, S. Adams, J. M. McCaffery, M. G. Farquhar, M. S. Kulomaa, T. E. Machen, H.-P. H. Moore, and R. Y. Tsien, *Chem. Biol.* 7, 197 (2000).

¹³ W. H. Weintraub and T. E. Machen, *Am. J. Physiol.* 257, G317 (1989).

compartments. Bafilomycin pretreatment also blocked H^+ -pumping ability of the organelles, which could alter the magnitude of the pH responses elicited by NH_3/NH_4^+ treatment. ER and Golgi pH both increased immediately due to the rapid entry of NH_3 , which is in equilibrium with NH_4^+ in solution.¹⁴ Using pK 9.0 for the $NH_4^+ \rightarrow H^+ + NH_3$ reaction and knowing $[NH_4^+]$ from the amount added to the Ringer solution and assuming that NH_3 equilibrates equally across all cell membranes, β was calculated from the rapid increase in pH (extrapolated to time zero) during the switch from Ringer to NH_3/NH_4^+ -containing Ringer according to Eq. (3)^{13,14}:

$$\beta = [NH_4^+]/\Delta pH \quad (3)$$

We have used two approaches to measure the H^+ leak rates across organelle (ER and Golgi) membranes. One approach measures the leak out of ER and Golgi membranes in intact cells, while the second method can be used to quantitate both the leak into and out of organelles of plasma membrane-permeabilized cells. For experiments using intact cells, the rates of H^+ leak out of the cytosol and organelles were determined by measuring the pH recovery of these compartments from an acid load. Prior to each experiment, cells were pretreated for 2 hr with 500 nM bafilomycin (H^+ v-ATPase inhibitor) to ensure we eliminated the H^+ pump contribution and only measured H^+ permeabilities. In separate experiments, cytosolic pH was monitored with the pH-sensitive dye BCECF-AM, while ER and Golgi pH were monitored by the avidin-Flubi-2 method. The compartments were acid loaded by an extended 20-min treatment with 40 mM NH_4Cl Ringer. The long treatment was required because the Golgi appeared to have a low permeability to NH_4^+ .¹² After washout of the NH_4Cl -containing Ringer with Na-free Ringer [Na^+ was replaced with *N*-methyl-D-glucamine (NMG)], the pH values of all three compartments typically acidified to pH < 6.4 and remained acidic, probably because the lack of Na^+ prevented the Na^+/H^+ exchanger in the plasma membrane from recovering the cytosolic pH. The H^+ leak rates out of the cytosol, ER, and Golgi were then measured when the Na⁺-free Ringer was replaced with Na⁺-containing Ringer. By comparing rates of H^+ leak out of the ER and Golgi, insights can be gained into the relative "leakiness" or permeability of these organelles to H^+ . This approach, which should be applicable to other organelles in which steady state pH is determined by countering activities of H^+ v-ATPase(s) and H^+ leak(s), is advantageous because cells and organelles remain in their intact state, and rates of H^+ leak are performed under conditions in which the transorganelle membrane pH (i.e., from organelle to cytosol) is always the same. A drawback to this method is that it allows conclusions only about

¹⁴ A. Roos and W. F. Boron, *Physiol. Rev.* **61**, 296 (1981).

relative H^+ leaks because the rate of pH recovery will always be limited by the rate of pH recovery due to plasma membrane mechanisms. In addition, the method requires controls to assure that the leak and pump are not affected by the presence or absence of Na^+ .

The second approach we used to study the H^+ leak across organelles required selective permeabilization of the plasma membrane, using streptolysin-O (SL-O), and then establishment of pH gradients across the ER and Golgi membranes. This method allowed us to monitor both the H^+ leak into and leak out of the organelles. SL-O is a bacterial toxin that binds cholesterol and forms pores at 37° . We used SL-O to selectively permeabilize the plasma membrane of cells by using the following protocol. One hundred microliters of reconstitution buffer [10 mM HEPES (pH 7.2), 10 mM dithiothreitol (DTT), 0.1% (w/v) BSA] was added to lyophilized SL-O (from S. Bhakdi, University of Mainz, Germany) to give a 1-mg/ml stock solution. HeLa cells expressing AV-KDEL or ST-AV were loaded with Flubida-2, chased in normal growth medium, and pretreated with bafilomycin (500 nM, 2 hr). The cells were rinsed twice with ice-cold Ringer before a 15-min incubation (on ice) in cold SL-O (5 mg/ml)-Ringer solution. The cold incubation allowed SL-O to bind to plasma membrane cholesterol without pore formation. Excess, unbound SL-O was removed by washing cells twice with ice-cold Ringer, and permeabilization was induced by incubating cells in a pH 7.4 intracellular buffer (IB consisted of, in mM: 110 potassium gluconate, 20 KCl, 0.1 $CaCl_2$, 2.7 K_2HPO_4 , 10 HEPES, 10 MES, 10 glucose, 5 Mg-ATP, 2 Na-GTP, 2 magnesium acetate, titrated to different pH values with NMG base) for 15 min at 37° to allow pore formation. We confirmed plasma membrane permeabilization of cells at the end of each experiment by treating the cells with 1 μM propidium iodide, which bound to DNA and turned nuclei red only in permeabilized cells. Because the efficiency of SL-O permeabilization is cell type dependent, the amount of toxin should be titrated for each different cell type.

After the Flubi-labeled, bafilomycin-pretreated cells were permeabilized with SL-O, we measured the H^+ leak into the ER and Golgi by establishing transmembrane pH gradients by changing the outside solution from pH 7.4 IB to pH 6.0 IB. The H^+ leak out of the membranes was determined by changing the outside solution from pH 6.0 IB to pH 7.4 IB. Using this protocol, we could also test whether counterions (such as K^+ and Cl^-) were required for the H^+ leak into and out of the organelles. In the ion replacement experiments, all chloride was replaced with gluconate and all potassium replaced with NMG to make Cl^- -free and K^+ -free IB solutions, respectively. For both the intact and SL-O permeabilized experiments, we were able to quantitate the H^+ leak into or out of the different

compartments by fitting the data to exponential equations and obtaining rate constants and half-times for the pH recoveries.

The advantages of the permeabilized cell approach are that it allows more quantitative measurement of H^+ leak (independently of plasma membrane pH regulation) and better control of ionic conditions. The disadvantage is that despite the fact that SL-O permeabilization was performed to minimize damage, this procedure could have induced subtle changes in H^+ permeability or resulted in the loss of important cytosolic regulatory factors. However, because Golgi membranes of permeabilized cells still responded to NH_3 and still maintained an acidic pH of <6.5 when not pretreated with bafilomycin (data not shown), SL-O did not seem to grossly alter organelle membranes.

Conclusion

We developed a novel method for measuring pH in specific intracellular organelles. Avidin chimera proteins were localized to specific compartments by appending organelle-specific targeting sequences to avidin. Cells expressing the organelle-specific avidin chimera proteins were loaded with Flubida-2, a membrane-permeable, pH-sensitive fluorescein-biotin derivative. Flubi-2 accumulated specifically and stably in avidin-containing organelles, allowing us to monitor steady state pH. Although there were several potential drawbacks of this method, none became problematic in our experiments. The presence of avidin in the cells (which might have been expected to bind all cellular stores of biotin and kill the cells) did not affect either viability or survival of the cells, even in stably transfected cells (M. Wu, K. Teter, and H. P. Moore, unpublished observations, 1999). Thus, it was not necessary to add extra biotin to the medium to counter the presence of avidin in the cells. In some cases, avidin chimera proteins were mislocalized, probably due to extended oligomerization of both the targeting domains and the avidin domains of the chimera proteins, but we were able to rescue the mistargeted proteins by coexpression of soluble avidin. Finally, control experiments indicated that pretreatment of cells with biotin-free medium did not improve labeling of cells with Flubi-2 (J. Llopis, unpublished observations, 1999).

The targeted avidin-Flubi approach was advantageous because it allowed specific targeting of a ratiometric pH-sensitive dye to the ER and Golgi of mammalian cells (as well as other compartments; M. Wu, T. E. Machen, and H.-P. Moore, unpublished observations, 1999). The method provides flexibility in that the Flubi dyes could be modified chemically to provide different pH sensitivities that would be suitable for making

measurements in both neutral organelles (e.g., ER) as well as in organelles that may vary in acidity from pH 6.4 (e.g., Golgi) to pH 4.5 (lysosomes). Using this method, we have performed a comparative study of pH regulation between the ER and Golgi of HeLa cells.¹² Fluorescence ratio imaging experiments can be performed on Flubi-loaded, avidin chimera protein-expressing cells under conditions in which the cells are SL-O permeabilized and/or pretreated with pharmacological agents (bafilomycin, brefeldin A). Fluorescence measurements can be made in any compartment that can retain an avidin chimera protein, and in any cell type that can express the proteins.

Additional Applications

The targeted avidin-biotin indicator method we have described in this chapter can be modified to study physiological events or processes other than pH regulation. To demonstrate this versatility we labeled cells expressing AV-KDEL with an NBD-biotin conjugate (Fig. 4), which proved to diffuse across cell membranes. The staining correlated with ER markers and was indistinguishable from that obtained with Flubi-2, except that the fluorescence was blue. Thus, biotin conjugates of fluorophores or fluorescent indicators other than fluorescein can potentially be made in order to label organelles with other colors (for dual-staining procedures) or to study their function in living cells. Cell lines developed expressing targeted avidin could thus be used for other purposes beyond monitoring organelle pH.

Acknowledgments

We thank Marilyn Farquhar and the ICC/EM Core Facility at UCSD (NIH Grant CA58689). We also thank George Oster, Michael Grabe, Hongyun Wang, and members of the Machen, Moore, and Tsien laboratories for helpful discussions.